At no order is there a requirement on $\langle\psi_k^{(0)}|\psi_k(l)\rangle$, so these quantities may be adjusted to yield

$$\langle\psi_j^{[L]}|\psi_k^{[L]}\rangle = \delta_{jk} + O(\lambda^{L+1}) .$$

---

*Sponsored by the National Science Foundation under Grant No. GP-6436. Research has benefited from facilities made available by the Advanced Research Projects Agency through the Center for Materials Research at Stanford University.

†NSF Predoctoral Fellow. Present address: Department of Chemistry, Jackson State College, Jackson, Miss. 39217.

‡Stanford Chemistry Department Fellow. Present address: Department of Neurology, Columbia College of Physicians and Surgeons, New York, N.Y. 10032.

[1]See, for instance, N. F. Mott and H. S. W. Massey, The Theory of Atomic Collisions (Oxford University Press, New York, 1965), p. 802 ff.

[2]A. Messiah, Quantum Mechanics (John Wiley & Sons, Inc., New York, 1962), Vol. II, p. 739 ff.

[3]T. Kato, J. Phys. Soc. Japan 5, 435 (1950).

[4]Total time derivative d_t is used because Ψ depends on t both directly and through σ.

[5]At present, it is not worth the effort to delineate properties of $H(\sigma)$ which insure conditions (1) and (2). In computational applications they may be verified explicitly.

[6]By definition, $\|f\| = \langle f|f\rangle^{1/2}$, etc.

[7]T. Kato, J. Fac. Sci. Univ. Tokyo Sec. I, 6, 145 (1949).

[8]E. C. Kemble, Quantum Mechanics (Dover Publications, Inc., New York, 1958), p. 178 ff.

[9]R. H. Young and W. J. Deal, Jr. (to be published).

[10]More precisely, $(1-P)\mathcal{H}$ is a subspace of $(1-P')\mathcal{H}$, where $\mathcal{H}$ is the full Hilbert space and P' is the projector for true eigenfunctions in S. The latter manifold reduces $H(\sigma)$, and $H-E_k$ has an inverse whose domain is everywhere dense in $(1-P')\mathcal{H}$ and therefore in $(1-P)\mathcal{H}$.

[11]Whether or not it does in a particular case is (in principle) a matter for computation. If it does not, one may be able to find an approximate solution to (8), in which case the final error expression becomes more complicated.

[12]For a discussion of (24), see Appendix D.

[13]J. Frenkel, Wave Mechanics, Advanced General Theory (Clarendon Press, Oxford, England, 1934), p. 253.

[14]A. D. McLachlan, Mol. Phys. 8, 39 (1964).

[15]L. R. Ford, Differential Equations (McGraw-Hill Book Co., Inc., New York, 1955), pp. 122–3.

[16]See, for instance, J. O. Hirschfelder, W. Byers Brown, and S. T. Epstein, Advan. Quant. Chem. 1, 255 (1964).

PHYSICAL REVIEW A VOLUME 1, NUMBER 2 FEBRUARY 1970

Multiple-Region Hydrogen Maser with Reduced Wall Shift*

E. E. Uzgiris† and N. F. Ramsey

Lyman Laboratory of Physics, Harvard University, Cambridge, Massachusetts 02138

(Received 7 July 1969)

The magnitude of the atom-wall collision frequency shift in the hydrogen maser has been reduced tenfold by confining the hydrogen atoms in a Teflon-coated cylindrical vessel that is 5 ft long and 5 ft in diam. The wall shift of this large maser was measured to be $-(2.3\pm0.8)\times10^{-3}$ Hz at 27 °C. Oscillation is achieved by a prestimulation method in which radiant atoms that have been prestimulated in the high rf field of one microwave cavity maintain a maser oscillation in a second cavity. A signal is extracted from the low-level cavity, amplified to a suitable value, and coupled into the high-level cavity to maintain the rf field there. A detailed theory of a multiple-region maser system is presented.

I. INTRODUCTION

The central feature of the hydrogen maser is the storage technique in which atoms are confined for up to a second in a region of constant rf phase in a resonant cavity and are thereby induced to radiate.[1–3] Unavoidably, the atoms must undergo many collisions with the surface walls of the containing vessel. Forces present on the atom during a wall collision perturb the energy levels of the atom and produce a phase change in the oscillating superposition state. The rate at which this phase

shift accumulates determines the departure of the maser output from the free-space hyperfine transition frequency. This wall effect has been the principal limitation of the hydrogen maser oscillator in absolute time and frequency measurements.[4]

The goal of the experiment described in this paper was to reduce the frequency shift associated with atom-wall collisions in the hydrogen maser. The diminution of the wall effect was obtained by a tenfold increase in the linear dimensions of the hydrogen storage vessel and thereby a corresponding decrease in the wall collision rate. Although the approach to the problem was a direct one, its implementation required a novel atom prestimulation technique for achieving maser oscillation. With this technique, oscillation is maintained in one microwave cavity by radiant atoms that are prestimulated in a second cavity. More generally, the prestimulation method, so central in this experiment, may be useful in other instances of a very small filling factor.

The frequency stability of one hydrogen maser compared to another has been as high as 7 parts in 10^{15} (for 1000 sec averaging times).[5] However, the absolute frequency of a hydrogen maser is determined with far less precision due to uncertainties of the wall effect. In some measurements,[6-8] the absolute frequency was uncertain by 5 parts in 10^{13}, and in others[4] by 3 parts in 10^{12}. Higher accuracies are difficult to achieve because of variations in wall-coating material from bulb to bulb. Thus, to achieve the full potential of the hydrogen maser in absolute time and frequency measurements, it is imperative that the wall effect on the maser output frequency be reduced.

One possible approach is to improve on the current wall material, FEP Teflon. But a reduction can be obtained straightaway by confining the atoms in a large Teflon-coated vessel and reducing their wall collision rate. If a superior wall surface were to be found, it could be used in this system as well to give still a further enhancement. In this experiment, radiating hydrogen atoms are stored in a cylinder 5 ft in diam and 5 ft long which gives a tenfold reduction in the wall collision rate over a 6-in.-diam storage bulb used in the conventional hydrogen maser.

Despite the reduction in the wall shift the problem of accurate measurement remains. Presently, experiments to measure the absolute wall effect involve comparing hydrogen masers with different bulb sizes. This method is limited in accuracy because of difficulties in obtaining reproducible surfaces and variations of surface quality from bulb to bulb.[9] Of course, the use of large bulbs, as in this work, should still yield higher accuracies of the wall effect. However, the 5-ft storage bulbs are unwieldy objects, difficult to coat and difficult to handle. A more promising technique involves the use of a flexible geometry which would allow a change of the atom mean free path between wall collisions without the necessity of changing bulbs of different size and possibly differing surface composition.[10]

The hydrogen-maser storage bulbs previously have been limited to about 6 in. diam in order that they occupy a region of constant phase in a microwave cavity determined in size by the requirement that it resonates in a TE_{011} mode at the hydrogen hyperfine transition frequency (1420 MHz). By placing most of the atom-containing volume outside the cavity, this restriction of size can be overcome, but not without a severe reduction in the filling factor.[11] Since this represents, equivalently, a severe reduction in the induced emission rate for the same given rf energy stored in the cavity, oscillation would be possible in such a system only if the cavity Q factor was inordinately high or if the hydrogen flux was prohibitively large. The former is experimentally unattractive, and the latter is not possible due to hydrogen-hydrogen collision effects.[3,12]

However, both of the above problems can be avoided through the method of prestimulation in a second cavity. In the large storage-box maser, two resonant cavities, each of which contains a conventional quartz storage bulb attached to the large chamber allowing atoms to flow freely in and out, are coupled together with an amplifier. Thus, a much higher oscillation level is maintained in one cavity than in the other. The strong field induces atoms into a radiant state, and, as a result, such radiant atoms are able, at a later time in their confinement history, to emit at an enhanced rate in the low-level cavity.

Prestimulation of the atoms by the strong field of the driving cavity is the central feature of this experiment, because the resulting increased emission rate in the low-level cavity allows self-excited oscillation at normal hydrogen fluxes and at normal cavity Q values. High-frequency stability can be obtained provided that the phase changes of the coupling line and amplifier are made small by appropriate means.

Earlier reports[13] of this work described the operating parameters of the large maser and gave some preliminary experimental results. In this paper, the multiple-region maser system is examined in detail and, in particular, the effects of interchamber flow are described. Section II contains a general description of the experiment and a restatement of the parameters derived in the earlier reports. In Sec. III, the problem is treated more generally, and the consequences of restricted flow are displayed. A description of the more important apparatus details appears in Sec. IV, and the results and discussion appear in Sec. V.

II. PRELIMINARY CONSIDERATIONS

A. Description of Experiment

The main features of the experiment are shown in Fig. 1. Although similar in many ways to the conventional hydrogen maser, the large maser differs fundamentally in that it utilizes prestimulation of atoms in the high rf field of one cavity to maintain an oscillation in the other. Of course, the large storage vessel in which the atoms spend most of their time and which provides a reduction in the wall collision rate is the other difference from the normal case. No significant departures of maser performance result in this system if the volume exchange rate is high. However, when the interchamber flow is restricted, certain new effects appear, which will be described in Sec. III.

Atomic hydrogen is produced by an rf discharge source, is state-selected by a hexapole magnet, and is confined for about 10 sec in the three interconnected chambers. The large chamber is a TFE Teflon-coated aluminum cylinder approximately 60 in. in diam and 60 in. in length. Two resonant cavities containing the small storage bulbs are coupled together through a high-gain rf amplifier (usually at about 90 db when oscillating). A signal at the hyperfine transition frequency is then extracted from the low-level cavity, amplified, and sent into the high-level cavity to maintain the field there. To minimize leakage through the junction points of the different storage vessels, the cavities, as well as the large chamber, are placed in a high vacuum of better than 10^{-6} Torr maintained by a pump that also removes the unfocused hydrogen released by the atom source. A separate pump maintains a background pressure of about 2×10^{-8} Torr in the storage volumes themselves. The entire vacuum vessel, with the exception of the pumps and source assembly, is placed in a three-layer magnetic shield enclosure so that magnetic relaxations due to gradients in the field would not be significant in a 10-sec storage time.

B. Effect of Prestimulation

Either the weak or the strong oscillating field induces the atoms to radiate and puts them in an energy-superposition state that oscillates in phase with the stimulating field. The random nature of flow of the atoms into the large zero-field chamber is not important as long as the phase memory is preserved. This is the case, since the T_2 relaxations are considered to be sufficiently long, so that the intermittent nature of the oscillatory field experienced by the atom in its confinement introduces no difficulties in the stimulated emission process. In this case, however, what is important at a particular time for the probability of emission by an atom is its prestimulation. An atom that has experienced only the weak-field region will radiate at a later time at a smaller rate than an atom that has also experienced the strong field. Thus, until the atoms experience the strong field, their contribution to the oscillation is negligible.

The effect of prestimulation can be readily demonstrated by an appeal to the classical vector model of a magnetic moment in an oscillatory field, as in magnetic resonance. The magnetic moment associated with the atomic spin is initially parallel to the static field H_0, and an oscillatory field is then applied that is perpendicular to H_0. In a rotating coordinate system,[14] the static field disappears at resonance and the moment precesses around the suitable stationary component of the oscillating field. In the usual approximation, the oppositely rotating-field component that makes up the oscillatory field is neglected because it is far off resonance. The rate of energy extraction from the spin system for $M=-\gamma\hbar J$ is then given by

$$P=\gamma\hbar J H_0 \sin\theta \frac{d\theta}{dt} , \tag{1}$$

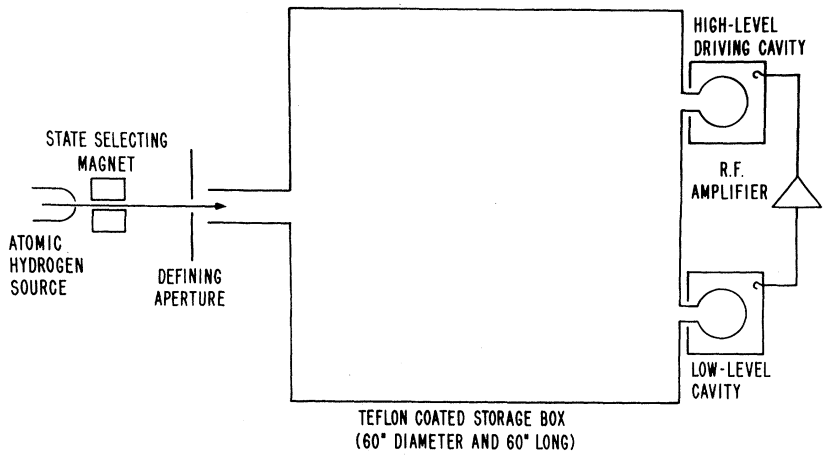

FIG. 1. Schematic diagram of the large hydrogen maser.

which, for a given rate of precession, is far greater when the spin is nearly perpendicular to H_0 than when it is nearly aligned with H_0. This enhancement is the prestimulation effect.

C. Oscillation Conditions

The degree of enhancement provided by the amplification in the two-cavity system is best described by deducing the conditions for oscillation. It is clear that the amplification will reduce the flux requirements, since part of the work of maintaining a suitable stimulating field is taken over by the amplifier. It is also not difficult to see that for this system the ratio of emitted power in the two cavities is proportional to the ratio of the field amplitudes, not only in the case of 90° prestimulation, but also at low-oscillation levels as well. The basis for this argument is that it is the strong field that determines the equilibrium oscillating magnetization and that the extraction of power from this magnetization is proportional to the amplitude of the stimulating rf field.[15]

A satisfactory description of the large storage-box maser can now be obtained by assuming a simplified model in which the atoms are allowed to enter each of the cavity regions many times.[13] An average rf field amplitude (in frequency units, i.e., $x=\mu_0 H/\hbar$) can be defined as

$$x=x_D V_D/V_T + x_L V_L/V_T , \tag{2}$$

where V_T is the total volume of the three storage regions and is very nearly equal to V_B, the volume of the large storage chamber alone, V_D is the driving-bulb volume, and V_L is the low-level bulb volume. Since we assume $x_D \gg x_L$ and $V_L \simeq V_D$, we neglect the low-level field contribution. This average field can be viewed as being applied continuously, and the analysis of the normal maser can be taken as a whole to deduce the total emitted power.[2,3] Of this total, most is radiated in the driving cavity, but a fraction, given by the field amplitude ratio, is radiated in the low-level cavity where the self-excited oscillation is maintained. The underlying assumption in this case is that because of the high amplification it is predominantly the driving field alone which determines the equilibrium value of the oscillating atomic magnetization.

Hence, the radiated power in the low-level cavity is

$$P_L = \frac{I\hbar\omega V_L}{4RV_D} \frac{x^2}{\gamma_1\gamma_2 + x^2 + (\gamma_1/\gamma_2)(\omega-\omega_0)^2} , \tag{3}$$

where $R=x_D/x_L$, I is the total hydrogen flux, and γ_2 and γ_1 are the usual relaxation rates ($\gamma_1 = T_1^{-1}$ and $\gamma_2 = T_2^{-1}$). As will be shown by the detailed treatment in a later section, this result holds as long as flow-constriction effects are negligible (i.e., volume interchange rate much higher than the relaxation rates).

In Ref. 13, the threshold flux for oscillation and the oscillator quality parameter q are derived in a straightforward calculation once the radiated power in the low-level cavity is established. The threshold flux is given by

$$I_{\text{th}} = \left(\frac{1}{R}\frac{V_B^2}{V_D^2}\right) \frac{V_L{}^c \hbar}{\mu_0{}^2 2\pi\eta_L Q_L T_t^2} , \tag{4}$$

where the subscript L refers to the low-level cavity, subscripts B and D to the zero-field and driving-field regions, respectively, $T_t^2 = \tau_1\tau_2$, the relaxation times when spin-exchange relaxation is zero, Q_L, $V_L{}^c$, and η_L are the low-level cavity quality factor, cavity volume, and bulb-filling factor.

Except for the parentheses, the expression is identical to the result for the normal case. It indicates that, if the lifetimes are increased by the same factor of 10 as the linear dimensions of the storage box, and if the amplifier gain is such that $R=V_B/V_D$, then despite the great loss in over-all filling factor the threshold flux is increased only by a factor of 10.

Also in Ref. 13, spin-exchange effects are considered and an oscillator quality parameter is derived that differs from the small maser case by the parentheses term,

$$q = \left(\frac{1}{R}\frac{V_B}{V_D}\right) \frac{V_L{}^c \hbar T_b \sigma \bar{v}_r I}{V_L \mu_0{}^2 \eta_L Q_L T_t 8\pi I_{22}} . \tag{5}$$

Here I_{22} is the flux in the $F=1$, $M_F=0$ state, σ is the spin-exchange cross section, T_b is the mean time the atom is in the system before escaping, and $\bar{v}_r$ is the average relative atom velocity. Because the quality parameter must be less than 0.172 for oscillation to occur,[3] the parentheses term must be unity or less indicating that the minimum required gain is of the order of V_B^2/V_D^2. In the specific instance of this large maser the minimum gain is approximately 70 dB. However, in practice, the required gain for oscillation was above 80 dB because the other parameters in Eqs. (5) and (4) were not entirely equivalent to the usual achieved values of the small masers.

D. Wall Shift

A hydrogen atom colliding with a wall surface can undergo one of several interactions: (a) It can engage in a chemical reaction with the surface

molecules[2]; (b) it can exchange spins with an unpaired electron spin on a particular wall site[16]; (c) it can be absorbed and suffer magnetic relaxation from the nonuniform magnetic fields of the nuclear spins on the surface[17]; or (d) it can simply experience a slight perturbation of the hyperfine constant as a result of the electron-cloud distortions induced by the van der Waals forces[2] and the Pauli exclusion principle. The first two processes contribute to the linewidth but not to frequency errors[18]; however, the last two interactions can produce frequency offsets and their effects must be measured.

As far as frequency shifts are concerned, a particular surface can be characterized by a phase shift per collision, Φ, that produces a frequency departure from the case of zero collisions given by

$$\delta\nu_W = v\Phi/2\pi d, \tag{6}$$

where v is the average atom velocity and d is the mean free path between wall collisions.

The quantity d can be calculated simply from the geometry.[19] Thus, the quantity Φ characterizing the surface can be deduced by measurement of the frequency offset of two masers with two different diameter bulbs. Internal consistency in a series of measurements determines whether the assumption about the equivalence of the coatings is valid or not. Alternatively, as stated above, a single bulb can be used if its geometry can be changed to vary the mean free path.

The large maser has a calculated mean free path of 38.3 in., whereas the typical bulb of 6 in. diam has a 4-in. mean free path.

E. Maser Tuning

The effects of cavity tuning are derived in Ref. 13 from the requirement of stability and self-consistency for the phase of the oscillating field. The result is identical to the one derived here in Sec. III through a circuit analog calculation of the two-cavity system. The tuning of either cavity can be varied, or the phase length of the amplifier loop can be changed to find a density-independent frequency. In the normal maser, this frequency after corrections for the magnetic field offset, second-order Doppler shift, and wall shift is the undisturbed hydrogen hyperfine frequency. At the density-independent tuning, the cavity is mistuned by just the amount needed to cancel the spin-exchange shift[18] since the spin-exchange shift is proportional to T_2^{-1}. In Sec. III, we show that for the large maser the spin-exchange shift can average in a different way so that a density-independent frequency no longer corresponds exactly to the true hyperfine valve but has certain small additional offsets. Those, however, can be measured and the frequency can be corrected with sufficient accuracy to the true unperturbed value.

III. THEORY OF MULTIPLE-REGION MASER

A. Introduction

In order to describe the effect of the separate regions and the interchamber flow in the large two-cavity hydrogen maser, it is necessary to formulate the problem in terms of the density-matrix technique.[20,21] The hydrogen-atom density-matrix equations of motion and their solutions have been obtained for the case of the conventional one-cavity and one-bulb maser.[12,18] At the price of more cumbersome algebra, this treatment can be extended to the large-maser case since in each of the regions the equations of motion of the density matrix can be specified and the equations can be coupled through the atom interchamber flow rates.

The spin-space density matrix for the ground state of hydrogen is defined as

$$\rho \equiv \begin{array}{c} F, M_F \\ 1,1 \\ 1,0 \\ 1,-1 \\ 0,0 \end{array} \begin{array}{c} \begin{array}{cccc} 1,1 & 1,0 & 1,-1 & 0,0 \end{array} \\ \begin{bmatrix} \rho_{11} & \rho_{12} & \rho_{13} & \rho_{14} \\ \rho_{21} & \rho_{22} & \rho_{23} & \rho_{24} \\ \rho_{31} & \rho_{32} & \rho_{33} & \rho_{34} \\ \rho_{41} & \rho_{42} & \rho_{43} & \rho_{44} \end{bmatrix} \end{array} . \tag{7}$$

The rate of change of this matrix is the sum of the rate of flow, rate of spin-exchange, rate of relaxation, and the rate of radiation.[12,22] These can be specified for each chamber of the large maser. Moreover, since the radiation field connects only one pair of states, there is only one set of nonzero skew elements, and it is sufficient to solve for $\rho_{22} - \rho_{44}$ and ρ_{42} in each region. However, in the most general case, the rate of change of these two quantities is not independent of the other density-matrix elements. Both spin-exchange relaxation and magnetic relaxation contribute small terms which depend on the equilibrium value of ρ.[18] Since these terms are small and since they alter slightly quantities which need not be known precisely (power, threshold flux, quality parameter), it will be assumed for the great algebraic simplification which results that no coupling occurs to the two diagonal elements ρ_{11} and ρ_{33}. The very precise description of the maser oscillator frequency does not suffer in this approximation because the nonunique terms of the complete density-matrix solution disappear in the determination of a density-independent frequency.[18] Moreover, in the case of low hydrogen density and negligible magnetic relaxation, the troublesome terms vanish. This in practice can be approached in the

large maser due to its large volume and due to the option of operating at a higher static field, which has the effect of reducing the relaxation due to field gradients.

B. Joint Density Matrix

The two different characteristics of a particle of interest here are its spin state and its location in space (only to the extent of knowing which chamber the particle occupies). A description of two separate characteristics, a and b, is given by a joint state and a joint density matrix[21] $\rho^{(ab)}$. Two sets of orthonormal functions are used to define $\rho^{(ab)}$. Each column and row index corresponds to two indices (m, n) of the eigenstates u_m and v_n. The mean value of an operator of the (a) system, $\langle Q^a \rangle$, is obtained by multiplying Q^a by the unit operator of (b). Thus, we have

$$\langle Q^a \rangle = \mathrm{Tr} Q^a 1^b \rho^{(ab)}$$

$$= \sum_{m,m'} Q_{m'm}{}^a \Big(\sum_{n,n'} \delta_{n'n} \rho_{mn,\, m'n'}{}^{(ab)} \Big)$$

$$= \mathrm{Tr}_{(a)} Q^a \rho^a \quad , \tag{8}$$

where

$$\rho_{mm'}{}^a = \sum_n \rho_{mn,\, m'n}{}^{(ab)} = (\mathrm{Tr}_{(b)} \rho^{(ab)})_{mm'} \, . \tag{9}$$

It is evident that $\rho_{mm'}{}^a$ represents the information on (a) alone.

If the states of the joint system are uncorrelated, that is, $\langle Q^a Q^b \rangle = \langle Q^a \rangle \langle Q^b \rangle$ for all pairs of Q, then the joint density matrix becomes a product,

$$\rho_{mn,\, m'n'}{}^{(ab)} = \rho_{mm'}{}^{(a)} \rho_{nn'}{}^{(b)} \quad . \tag{10}$$

The states of concern in the large-maser description are the space and the spin states. The joint matrix will be a product of ρ^{space} and ρ^{spin}, because we shall assume that the random motion of atoms in the chambers is uncorrelated (in the above sense) with the spin states. The space part of the joint matrix ρ^{space} will be a diagonal 3×3 matrix, the diagonal terms of which, $\rho_{jj}{}^{\mathrm{space}}$, will represent the probability of being in the jth chamber. (Here $j = B$, L, and D, where B is the large zero-field chamber, L is the weak-field chamber, and D is the driving-field chamber.) The off-diagonal elements vanish because we assume that interference terms go to zero when the deBroglie wavelength of the particle is much smaller than the macroscopic dimensions of the chambers.

We define

$$\rho^j = (\rho_{mm'}{}^{\mathrm{spin}})_j = \rho_{mm'}{}^{\mathrm{spin}} \rho_{jj}{}^{\mathrm{space}} \, . \tag{11}$$

For the expectation value of a spin operator, we have

$$\langle Q^{\mathrm{spin}} \rangle = \sum_j (\mathrm{Tr} \rho Q)_{\mathrm{spin}} \rho_{jj}{}^{\mathrm{space}}$$

$$= \sum_j \mathrm{Tr}_{\mathrm{spin}} \rho^j Q^{\mathrm{spin}} \, . \tag{12}$$

The properties that this joint operator $\rho = \rho^{\mathrm{spin}} \rho^{\mathrm{space}}$ must obey are

$$\rho = \rho^{\dagger} \, , \tag{13a}$$

$$\mathrm{Tr} \rho = \sum_j \mathrm{Tr}_{\mathrm{spin}} \rho^j = \sum_j \rho_{jj}{}^{\mathrm{space}} = 1 \, , \tag{13b}$$

$$\rho_{mm}{}^{\mathrm{spin}} \rho_{jj}{}^{\mathrm{space}} = \rho_{mm}{}^j > 0 \, . \tag{13c}$$

It is a straightforward matter, by application of the Schrödinger equation, to show that

$$\frac{\partial}{\partial t} \rho^j = \frac{i}{\hbar} [\rho, H]^j \quad , \tag{14}$$

where H^j is the spin Hamiltonian of the jth volume.

C. Equations of Motion

We can now write the rate equations for each of the three ρ^j operators, just as in the single-volume case. In each region, the time rate of change of ρ^j will include the flow of atoms into and out of that region, the effects of relaxation, the effects of hydrogen-hydrogen collisions, and the effects of the rf field:

$$\frac{d}{dt} \rho^j = \frac{i}{\hbar} [\rho, H]^j + \frac{d}{dt} \rho_{\mathrm{se}}{}^j + \frac{d}{dt} \rho_{\mathrm{relax}}{}^j + \frac{d}{dt} \rho_{\mathrm{flow}}{}^j \, . \tag{15}$$

We assume the relaxations are the same in all regions and that they can be separated into T_1- and T_2-type components. In the absence of off-diagonal elements other than the two connected by the hyperfine transition, we can solve for the equilibrium values of the population difference $\rho_{22}{}^j - \rho_{44}{}^j$ and each of the oscillating off-diagonal elements $\rho_{42}{}^j = \rho^*{}_{24}{}^j$ in each region. We designate

$$\rho_{22}{}^D - \rho_{44}{}^D = D_D; \quad \rho_{22}{}^L - \rho_{44}{}^L = D_L;$$

$$\rho_{22}{}^B - \rho_{44}{}^B = D_B; \quad \rho_{42}{}^L = L_{42};$$

$$\rho_{42}{}^{D} = D_{42}; \quad \text{and} \quad \rho_{42}{}^{B} = B_{42} \ . \tag{16}$$

In the large zero-radiation field chamber we have for the population difference

$$\frac{d}{dt} D_B = \tfrac{1}{2}\gamma_e - \gamma_{1B} D_B + \gamma_{LB} D_L + \gamma_{DB} D_D \ , \tag{17}$$

where γ_e is the escape rate out of the large chamber and thus out of the storage regions, and γ_{LB} and γ_{DB} are the flow rates from the low-level cavity into B and from the driving cavity into B, respectively. The remaining term is $\gamma_{1B} = \gamma_1' + \gamma_H + \gamma_{BL} + \gamma_{BD} + \gamma_e$. Here γ_H is the spin-exchange relaxation rate,[23] γ_1' is the sum of the longitudinal relaxation rates excluding the escape rate and the exchange relaxation rate, γ_{BL} is the flow of atoms from B into L, and γ_{BD} is the flow of atoms from B into D. As a matter of convenience, we express all rates as γ's rather than as the inverse of the characteristic times.

For the rate of change of the off-diagonal term in B, we have

$$\frac{d}{dt} B_{42} = -\{\gamma_{2B} - i[\omega_0 - (\lambda/4\sigma)\gamma_H D_B']\} B_{42} + \gamma_{LB} L_{42} + \gamma_{DB} D_{42} \ , \tag{18}$$

where $\gamma_{2B} = \gamma_e + \gamma_2' + \frac{1}{2}\gamma_H + \gamma_{BL} + \gamma_{BD}$. Here the relaxation terms designated by the subscript 2 are, of course, the transverse relaxations, and the flow terms are as defined above. The imaginary part of the equation contains the spin-exchange frequency shift[18,24]

$$\omega_B' = \omega_0 - (\lambda/4\sigma)\gamma_H D_B' \ , \tag{19}$$

where D_B' is the spin-space population difference alone, $D_B = D_B' \rho_B{}^{\text{space}}$. Later we will also use the relationship $\Delta_B = \omega - \omega_B'$. The rf field is zero in the large chamber B, so there is no characteristic field term in Eq. (18).

In the weak-field region L, we have the two equations

$$\frac{d}{dt} D_L = \gamma_{BL} D_B - \gamma_{1L} D_L - 2x_L \operatorname{Im}(L_{42} e^{-i(\omega t + \theta)}), \tag{20}$$

and

$$\frac{d}{dt} L_{42} = \gamma_{BL} B_{42} - \{\gamma_{2L} - [\omega_0 - (\lambda/4\sigma)\gamma_H D_L']\} L_{42} + \tfrac{1}{2} i x_L e^{i(\omega t + \theta)} D_L \ , \tag{21}$$

where we identify the new terms as $\gamma_{1L} = \gamma_1' + \gamma_H + \gamma_{LB}$, and $\gamma_{2L} = \gamma_2' + \frac{1}{2}\gamma_H + \gamma_{LB}$.

In the driving field region D, we have

$$\frac{d}{dt} D_D = \gamma_{BD} D_D - \gamma_{1D}' D_D - 2x_D \operatorname{Im}(D_{42} e^{-i\omega t}) \ , \tag{22}$$

and

$$\frac{d}{dt} D_{42} = \gamma_{BD} D_{42} - \{\gamma_{2D} - i[\omega_0 - (\lambda/4\sigma)\gamma_H D_D']\} D_{42} + \tfrac{1}{2} i x_D e^{i\omega t} D_D \ , \tag{23}$$

where $\gamma_{1D} = \gamma_1' + \gamma_H + \gamma_{DB}$ and $\gamma_{2D} = \gamma_2' + \frac{1}{2}\gamma_H + \gamma_{DB}$. The rf fields in L and D are oscillating at the same angular frequency ω, which is required by the condition of stationary oscillation; however, we allow a phase difference θ between the oscillating fields. The phase difference will be solved for in Sec. III F.

In the usual method of quasistationary solution $\dot{D}_L = \dot{D}_D = \dot{D}_B = 0$, and the off-diagonal elements are $\rho_{42}{}^{j} = (\alpha_j + i\beta_j) e^{i\omega t}$. These equations reduce to nine coupled nonlinear algebraic equations. The solution of these equations is greatly simplified by keeping only first-order terms in the frequency deviation from resonance. The oscillation is assumed nearly at resonance. If exact resonance is assumed, the nine rate equations would reduce to six since the three equations representing the real part of the off-diagonal elements which are linearly dependent on $(\omega - \omega')T_2$ would disappear. This, however, would provide insufficient information to describe cavity pulling or spin-exchange shift effects. The procedure[25] is to solve for the population difference and the imaginary part of the off-diagonal element in each region at resonance. Then, the remaining terms, the real part of the off-diagonal elements, are obtained by keeping $(\omega - \omega')T_2$ to first order and using the resonance values of the other density-matrix terms which depend on $(\omega - \omega')T_2$ only in second order and thus remain sufficiently accurate. A great simplification is also afforded in the equations by the fact that the atoms leave the smaller chambers at a much faster rate than any relaxation rate. That is to say, $\gamma_{LB} \simeq \gamma_{DB} \gg \gamma_1, \gamma_2$ even when the flow rate from B into L or D is comparable to γ_1 or γ_2. The ratio of the flow rates in the reverse directions is $\gamma_{LB}/\gamma_{BL} = V_B/V_L = r$, the volume ratio, which is about a factor of 10^3. Furthermore, it is very helpful also to realize that $x_D \gg x_L$, which is ensured by the high gain of the amplifier.

D. Solutions

If the off-diagonal element is represented as $\rho_{42}{}^{j} = (\alpha_j + i\beta_j) e^{i\omega t}$, and if we define $x^2/\gamma_{BD}{}^2 = \xi$, and if we also introduce an interchamber flow parameter

$$\kappa = (1+\gamma_1\gamma_{BD}^{-1})(1+\gamma_2\gamma_{BD}^{-1}) , \tag{24}$$

then the results are expressed as

$$\begin{aligned}
\rho_{42}^{L} &= \frac{1}{r}\rho_{42}^{B} = \frac{\gamma_e x(\Delta_B\gamma_2^{-1}+i)e^{i\omega t}}{4r(\gamma_1\gamma_2+x^2\kappa)} ,\\
\rho_{42}^{D} &= \frac{\gamma_e x[\Delta_B\gamma_2^{-1}+i(1+\gamma_2\gamma_D^{-1})]e^{i\omega t}}{4r(\gamma_1\gamma_2+x^2\kappa)} ,\\
D_L &= \frac{1}{r}D_B = \frac{\gamma_e\gamma_2(1+\xi)+\gamma_e\gamma_D\xi}{2r(\gamma_1\gamma_2+x^2\kappa)} ,\\
D_D &= \frac{\gamma_e\gamma_2}{2r(\gamma_1\gamma_2+x^2\kappa)} .
\end{aligned} \tag{25}$$

Here we have set the volumes of the two cavity bulbs equal since, in practice, it is advantageous to keep both near an optimum size. If the volumes differ, then a corrective factor, the ratio V_L/V_D, multiplies the solutions for the low-level region.

The main features of the density-matrix solutions are: (a) the space part of the joint density matrix is represented by the volume ratio factor r; (b) the limitations imposed by flow constriction from the large chamber into the driving chamber are represented by the κ term directly and by the ξ term indirectly; (c) the flow constriction into L, within certain limits, is not critical and is not a limiting factor; and (d) the resonant frequency of the system is determined by the average value in B, a fact which is represented by the dependence of the α's only on Δ_B. All these features, with the exception, perhaps, of the flow-constriction limitations, are reasonable. The theory of the separated oscillatory-field resonances for molecular beams indicates that it is the average energy spacings, including the region of no oscillating field, which determine the resonant frequency.[14] The probability of an atom being located in a certain chamber is on the average in the case of random motion, the ratio of the volume of that chamber to the total volume of the containing system. The flow into the weak-field region does not appear as a limitation because, whereas it is the driving-field cavity which determines the equilibrium values of the density matrix, those values are reflected in L as long as γ_{LB} is greater than γ_2 or γ_1, a condition easily met even if γ_{BL} is less than the relaxation rates. The term κ becomes nonunity when the flow rate into D becomes of the same order as the relaxation rates γ_1 and γ_2.

The solutions are, of course, approximate – mainly because they were obtained only near resonance. However, they will be of sufficient accuracy to allow the important predictions about the maser to be made.

E. Radiated Power and Oscillation Conditions

We must estimate the radiated power in the low-level cavity in order to deduce the oscillation conditions for the larger maser. In doing so we shall derive the important quality parameters to judge the condition of the maser oscillator and its range of oscillation.

In general the power released by the oscillating atomic magnetization will be given by

$$P = \langle \int \vec{M}\cdot\frac{d\vec{H}}{dt}dr^3\rangle , \tag{26}$$

where a time average of the power is taken.

In general, the magnetization can be written as

$$\vec{M} = (IT_b/V)g_J\mu_0\,\mathrm{Tr}\rho\vec{J} . \tag{27}$$

Thus, for the low-level cavity, we have

$$M_L^{\dagger} = (IT_b/2V_L)g_J\mu_0\rho_{42}^{L} . \tag{28}$$

By the dagger notation we mean an oscillating quantity A is separated as $A = A^{\dagger}e^{i\omega t}+A^{\dagger *}e^{-i\omega t}$. This notation will be used in several places below.

When this result is used in Eq. (26), the radiated power can finally be written as

$$P_L = (I\hbar\omega/4R)x^2/(\gamma_1\gamma_2+x^2\kappa) . \tag{29}$$

The effects of the flow constriction into the region of prestimulation are clearly evident in the κ term, which departs from unity when the rate of flow into the driving cavity becomes as small as the relaxation rates. In fact, the maximum radiation is reduced directly by κ because the field-amplitude terms in that case cancel. If n is the number of entries on the average into the strong field, then when that number is very small, the maximum radiation rate goes as

$$P_L = (I\hbar\omega/4R)n^2 . \tag{30}$$

This is reasonable, since most of the atoms in that case decay before contributing to the oscillating field. A degradation at low oscillation levels also takes place; however, it is not explicitly visible in the expressions above. To exhibit more clearly this flow-constriction effect, it is necessary to derive the oscillation conditions and the oscillator quality parameter.

As in the usual case, the radiated power is set equal to the power losses in the low-level cavity for oscillation to occur. We should note, however, that Eq. (29) is not entirely correct if there is a phase difference between the magnetization and the

field. This situation can arise in the large maser because of the presence of two cavities and the amplifier loop; it is discussed in detail in the section on cavity tuning below. If the phase difference is small, a case of most interest in practice, then the error is entirely negligible and we obtain from the oscillation requirement

$$(\omega k/Q_L{}^l x^2) = (I\hbar\omega/4R)x^2/W_L - (\omega/Q_L{}^l)\gamma_1\gamma_2 , \quad (31)$$

where $Q_L{}^l$ is the loaded cavity Q factor for the L cavity, and W_L is the stored energy.

We define

$$P_0 = I_{th}\hbar\omega/4R , \quad (32)$$

where I_{th} is the threshold flux defined in Eq. (4). This is the maximum radiation in the weak field possible from I_{th} flux of atoms into the large-maser system.

Equation (31) can be factored for terms dependent on flux, i.e., spin-exchange relaxation terms, and the flux dependence can be displayed:

$$\kappa P_L = \frac{I\hbar\omega}{4R} - [\Gamma_1\Gamma_2 + (\tfrac{1}{2}\Gamma_1 + \Gamma_2)\gamma_H + \tfrac{1}{2}\gamma_H{}^2](\omega/Q_L{}^l)W_L/x^2 . \quad (33)$$

Here Γ_1, Γ_2 are the usual relaxation rates when the spin-exchange relaxation is zero. Identifying the constant c,

$$c = 2(\tfrac{1}{2}\Gamma_1 + \Gamma_2)(\Gamma_1\Gamma_2)^{-1/2} , \quad (34)$$

and the important quality parameter q given in Eq. (5), we finally obtain the expression that displays the important flux dependence:

$$P_L/P_0 = (1/\kappa)[-2q^2(I/I_{th})^2 - (cq-1)I/I_{th} - 1], \quad (35)$$

where we have also used

$$x_L{}^2/W_L = (\mu_0{}^2/\hbar^2)(8\pi/V_L{}^c)\eta_L . \quad (36)$$

The effect of constriction, represented by κ, is now explicit for all flux levels: Radiated power is directly reduced by the κ factor. The oscillation range defined by q remains insensitive to flow effects. Since this range is defined by zero-power points, the insensitivity is not surprising. In practice, the levels are reduced by κ; in order to achieve some minimum oscillation level, a higher flux level is more necessary than in the case of negligible constriction. Moreover, if desired, the κ factor can be expanded into a second-order polynomial in flux, I, to give a complete description of the oscillation level as the flux is varied. However, the expression as it stands will be of sufficient detail for our purposes here.

F. Cavity Tuning

The effects of cavity pulling of the oscillation frequency have been described in Ref. 13 using the requirement of phase constancy. That result can be obtained by a rather direct approach in which we treat the resonant cavities as LCR series circuits.[26] An alternative and equivalent approach[25] is to describe each of the two cavities by an equation derived by Slater for a resonant cavity with a microwave circuit.[27] However, since in that analysis the explicit modification which allows the coupling of the two equations and the unique determination of the oscillation frequency of the large maser does not appear as clearly as in the discussion that follows, it will not be given here.

In the inductor of the LCR series circuit we assume a magnetization due to the oscillating atoms. The voltage across the inductor will be given by[28]

$$V^\dagger = i\omega K(H^\dagger + 4\pi\eta' M^\dagger) , \quad (37)$$

where K contains all the units and geometrical factors, η' is the filling factor multiplied by the ratio of bulb-to-cavity volume, and $H^\dagger$ and $M^\dagger$ are the z components and are averaged over the bulb volume.

The voltage drop around the entire LCR circuit loop must be zero. Thus, using several circuit identifications, in particular that $H^\dagger = K'I'$ (I' is the current), we obtain

$$iQ4\pi\eta' M^\dagger + H^\dagger\{1 + \beta' + iQ[(\omega/\omega_c) - (\omega_c/\omega)]\} = 0. \quad (38)$$

Here β' is the coupling coefficient for the power coupled out of the cavity. The second term is a familiar one describing a damped circuit, and the first term indicates the effects of the magnetization. On multiplying and dividing by the appropriate factors, we remove η' and are left with an expression identical to one used for the conventional maser case involving a complex Q_m factor.[29]

For the single-cavity maser, Eq. (38) is sufficient to determine the oscillation frequency. However, in the case of the two-cavity system of Fig. 1, we must account for the effect of the second cavity and the amplifier as well. In this situation, the phase of the two rf fields need not be the same and must not be assumed *a priori*. Through the use of a second expression similar to Eq. (37), it is possible to eliminate the unknown phase (this was done implicitly in the phase-constancy argument of Ref. 13), and to display a unique expression for the oscillation frequency.

We can take account of the unknown phase θ by specifying that $H_D{}^\dagger = (\hbar/\mu_0)^{\frac{1}{2}}x_D$ and $H_L{}^\dagger = (\hbar/$

$\mu_0)^{\frac{1}{2}}x_L e^{i\theta}$. Then for the driving cavity we add on an extra term on the left-hand side of Eq. (38) to represent the power input from the amplifier. After some manipulation we obtain

$$i4\pi\frac{M_D^{\dagger}H_D^{\dagger}V_D}{\langle\vec{H}^{\dagger}\cdot\vec{H}^{\dagger *}\rangle_D V_D{}^c}+\frac{1+\beta_D'}{Q_D}+i\left(\frac{\omega}{\omega_D}-\frac{\omega_D}{\omega}\right)$$

$$-\left(\frac{n_L}{n_D}\frac{K_D'}{K_L'}\right)\frac{\beta_D'}{Q_D}\frac{A_0}{R}e^{i(\phi+\theta)}=0\ . \qquad (39)$$

Here the n terms in the square bracket refer to the coupling of the cavities, i.e., $n^2=\beta'$ when the resistive impedance of the cavity equals the characteristic impedance of the transmission lines. The terms K' refer to the proportionality between the current in the analog circuit and the rf field amplitude. If the two cavities are similar, then the bracket term will be unity. (Note that the β' refers to cavity coupling as opposed to the unprimed β which refers to a density-matrix component.) The term $\vec{H}^{\dagger}\cdot\vec{H}^{\dagger *}$ is averaged over the whole cavity volume $V_D{}^c$. The voltage gain is A_0, and R is as defined in Eq. (3). The phase shift of the amplifier and transmission lines is explicitly represented by ϕ.

By using Eq. (38) and by noting that all quantities refer now to the L cavity and L bulb, we can eliminate θ from Eq. (39):

$$i\frac{4\pi M_D^{\dagger}H_D^{\dagger}V_D}{\langle\vec{H}^{\dagger}\cdot\vec{H}^{\dagger *}\rangle_D V_D{}^c}+\frac{1}{Q_D{}^l}+i\left(\frac{\omega}{\omega_D}-\frac{\omega_D}{\omega}\right)+if\frac{\beta_D'}{Q_D}e^{i\phi}\frac{Q_L{}^l 2\pi M_L^{\dagger}\hbar x_L V_L}{\mu_0\langle\vec{H}^{\dagger}\cdot\vec{H}^{\dagger *}\rangle_L V_L{}^c}\frac{1}{1+iQ_L{}^l(\omega/\omega_L-\omega_L/\omega)}=0\ . \qquad (40)$$

Here f stands for $n_L K_D' A_0/n_D K_L' R$, and Q^l is the loaded-cavity Q factor.

To simplify this expression further, we need to evaluate the terms involving the magnetization. From Eq. (28), we recognize that

$$M_L^{\dagger}=I(T_b/V_L)(\alpha_L+i\beta_L)\ . \qquad (41)$$

Using the results of the density-matrix calculation we obtain the relation

$$\frac{4\pi M_L^{\dagger}(\hbar/\mu_0)^{\frac{1}{2}}x_L V_L}{\langle\vec{H}^{\dagger}\cdot\vec{H}^{\dagger *}\rangle_L V_L{}^c}=\frac{P_L}{\omega W_L}(\Delta_B T_2+i)\ . \qquad (42)$$

A similar term involving the driving cavity D can be obtained by replacing the L subscripts with D subscripts. However, since $P_D/\omega W_D=(1/R)P_L/\omega W_L$, and R is of order 10^3 or higher (Sec. II), this term will be neglected in Eq. (40).

For the case when ϕ, $\Delta_B T_2$, and $Q_L{}^l(\omega/\omega_L-\omega_L/\omega)$ are small compared to unity, a situation of most practical interest, Eq. (40) becomes

$$\frac{1}{Q_D{}^l}+i\left(\frac{\omega}{\omega_D}-\frac{\omega_D}{\omega}\right)+if\frac{Q_L{}^l}{Q_D'}\frac{P_L}{\omega W_L}\times\left[\Delta_B T_2+i+Q_L{}^l\left(\frac{\omega}{\omega_L}-\frac{\omega_L}{\omega}\right)-\varphi\right]=0\ , \qquad (43)$$

where terms of second order in the small quantities are neglected. Here Q_D' represents the output Q factor.

The real part of this equation yields

$$P_L/\omega W_L=Q_D'/fQ_D{}^l Q_L{}^l\ . \qquad (44)$$

This, together with Eq. (29) when θ is small, indicates that

$$f=Q_D'/Q_D{}^l\ . \qquad (45)$$

Thus, for the case of critical coupling and identical cavity parameters, the voltage gain A_0 and the field amplitude ratio are related by $A_0=2R$.

The imaginary part of Eq. (43) yields the desired tuning expression

$$(\omega-\omega_B')T_2=Q_D{}^l(\omega/\omega_D-\omega_D/\omega)+Q_L{}^l(\omega/\omega_L-\omega_L/\omega)-\phi\ . \qquad (46)$$

The oscillation frequency is determined from this expression since ω on the right-hand side can be replaced with ω_0 with negligible error. There remains the important task of considering the departure of ω_B' from ω_0, due to spin-exchange collisions.

G. Spin-Exchange Frequency Shift

Equation (46) describes not only the pulling of the oscillator frequency by the cavities and the

amplifier, but also contains the effects of hydrogen-hydrogen collisions in the departure of the resonant frequency from ω_0. The frequency ω_0 is, of course, offset from the zero-magnetic-field hyperfine frequency by the shift of the energy levels due to magnetic field, the second-order Doppler effect, and the effect of wall collisions. These must be accounted for separately as described in several works.[2-5] However, the spin-exchange shift can be evaluated explicitly in terms of the density-matrix solutions and the collision parameters λ and σ as indicated by Eq. (19). The result after some rewriting is

$$\omega_B' - \omega_0 = -(\lambda/16\sigma)m'[(1+\xi)/T_2 + \xi/T_D] , \quad (47)$$

where $T_D = \gamma_D^{-1}$, and

$$m' = [(1/R)(V_B/V_D)]V_L^{\,c}\hbar v_r/\pi\eta_L\mu_0^{\,2}Q_L^{\,l}V_L . \quad (48)$$

The factor m' is related to the quality parameter q by $q = m'\frac{1}{8}(I/I_{22})T_b/T_t$, and it also appears in the requirement for oscillation to occur,

$$(\gamma_1\gamma_2 + x^2\kappa)^{-1} = \tfrac{1}{2}T_b T_H m' . \quad (49)$$

This latter result can, if desired, be used further to eliminate ξ in Eq. (47). However, it is just as instructive for this discussion to continue to display the power-dependent terms.

Thus, the output frequency of the large maser is determined by

$$\omega - \omega_0 = \left[2Q_L^{\,l}\left(\frac{\omega_L - \omega_0}{\omega_0}\right) + 2Q_D^{\,l}\left(\frac{\omega_D - \omega_0}{\omega_0}\right) + \phi - \frac{\lambda}{16\sigma}m'\right]\frac{1}{T_2} - \frac{\lambda m'\xi}{16\sigma T_2} - \frac{\lambda m'\xi}{16\sigma T_D} . \quad (50)$$

We have remarked earlier on the significance of the ξ terms in the density-matrix solutions. The terms evidently arise from flow-constriction effects which produce an equilibrium population difference in the zero-radiation field chamber that is different from the case of a continuous application of an rf field. An alternative statement is that a significant fraction of the incoming atoms never radiates if the flow rate into the stimulating field is of the same order as the relaxation rates.

In the conventional single-bulb maser, the last two terms of Eq. (50) are absent and the cavity tuning is varied until a density-independent frequency corresponding to ω_0 is achieved. Unfortunately, because of the presence of the power-dependent terms such a simple tuning procedure is no longer adequate here if absolute frequency of higher accuracy than several parts in 10^{13} is desired. For sizable constriction effects and high oscillation levels the term ξ can become of the order of unity, and an experimental measurement of the last two terms must be made. Under the achieved operating conditions of the large maser it is estimated that the neglect of the power terms produces an error of 1×10^{-13} on the determination of the hydrogen hyperfine frequency. Thus, a 50% measurement of this effect in this case would reduce the frequency uncertainty to a value of 5×10^{-14} and well below the errors associated with the other shifts of the hyperfine frequency.

Of course, another approach for the future is to increase the flow rate into driving field relative to the relaxation rates. The principal reason for the appearance of the constriction limit in the present work is due to not achieving the desired lifetime of 10 sec. A threefold longer lifetime would reduce the power terms from the present worst case by a factor of 10 and would make them negligibly small in frequency tuning. In addition, the coupling geometry of the driving bulb to the large chamber could be improved to give a flow enhancement over the present case. Either of these should give, therefore, an improvement on the effects of flow constriction and their limitation in frequency accuracy.

IV. APPARATUS

We concern ourselves here with some of the unique aspects of the large-maser apparatus. The state-selector magnet and the discharge source of atomic hydrogen are similar to previous descriptions[3] and will not be given here.

The central parts of the system shown schematically in Fig. 1 are the storage chambers and the two coupled microwave cavities. Both of the small storage bulbs are 6-in.-diam spherical quartz bulbs (made by U. S. Fused Quartz Co.). The driving cavity bulb has a 3-in.-diam neck by which it is connected to the large chamber as depicted in Fig. 2. Since the flow rate into the low-level region is far less critical and since rf leakage from one cavity to the other is a serious experimental problem, the other bulb has only a 2-in. neck opening. All surfaces, including the neck flange by which a butt seal to the large chamber is accomplished, are coated with FEP Teflon (Du Pont 120) in the usual way.[3]

The large chamber is an aluminum cylinder with $\frac{1}{8}$-in.-thick wall and 56 in. diam with a dished head on one end and a flat $\frac{1}{4}$-in.-thick plate on the other end. The extreme length dimension is 60 in. Three small ports and a manhole are located on the flat end plate. A 4-in.-diam pipe which mates to the pumpout pipe section is attached to the center port and serves to separate the storage chambers from the outer vessel. The geometrical lifetime

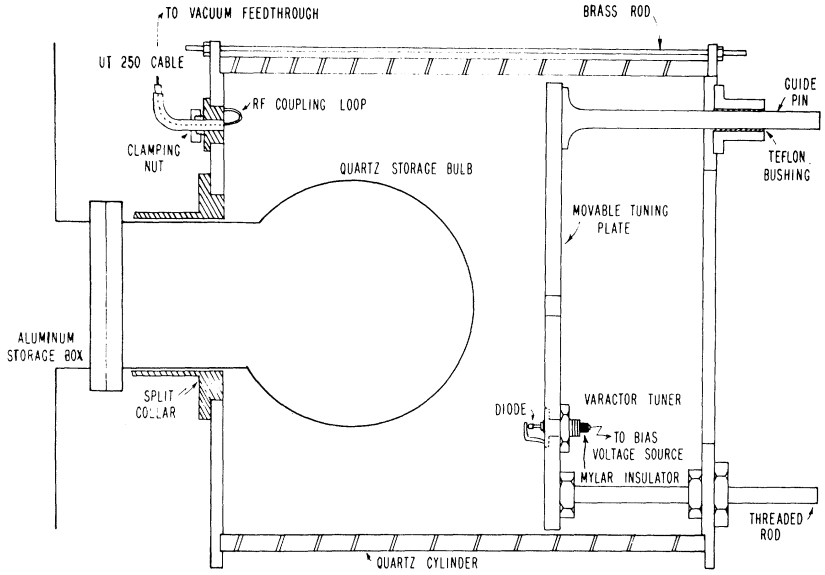

FIG. 2. Cavity assembly.

of the atoms in the confinement regions is defined by an aperture of suitable size placed on this 4-in. pipe after it has sealed to the lower pump section shown schematically in Fig. 3. Finally, in order to allow access into the interior for Teflon coating, a manhole is provided with a cover plate.

All storage-chamber seals are gasketless in order to avoid outgassing problems of Teflon gaskets, which are the only acceptable kind in regions open to hydrogen atoms. Because of the high vacuum in the vessel itself, moreover, some degree of leakage is tolerable as long as it is not excessive and as long as it does not significantly shorten the geometrical lifetime of the atoms. This appears to be the case in practice, since a pressure differential of nearly 2 orders of magnitude is

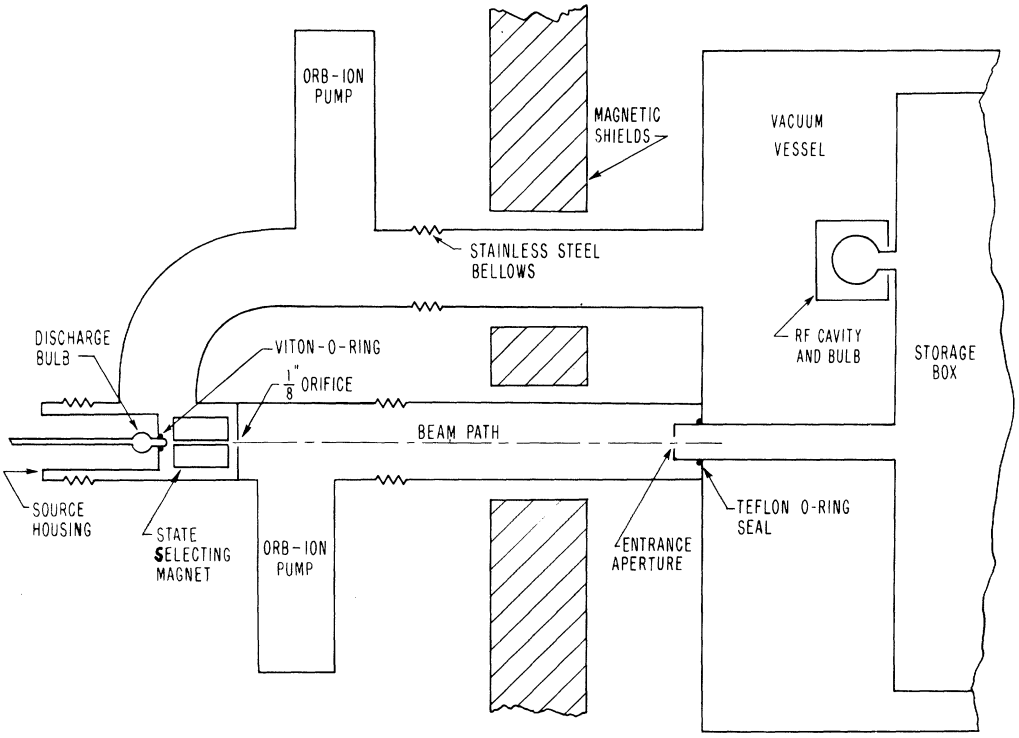

FIG. 3. Schematic view of the vacuum system.

maintained when the maser is operating.

The Teflon coating was done commercially (by Precision Coating Co., Dedham, Mass.). TFE Teflon was sprayed and then fused by baking for an appropriate time at 350 °C. The film thickness was built up to about 2 mils by repeating the coating process four times. The vessel was then given a visual inspection and a water drop test over several arbitrary interior areas before being washed with a Freon solvent and given one final cleaning bake.

The cavities are basically similar to ones used in earlier experiments,[3] but there are some differences: A large hole is necessary in the fixed end plate of the cavity to allow the bulb neck to pass through and attach to the large storage box; fine tuning is accomplished entirely by a varactor diode tuner device.

The cavity is provided with a split collar device which clamps around the bulb neck and extends from the cavity end plate where it is attached to the rear of the bulb neck flange. It reduces the 4.5-in.-diam hole in the plate, which is necessary to allow the bulb flange to pass through, to nearly the neck size of the bulb. This partial hole covering and the extension of the collar to the rear of the bulb flange as a wave guide beyond cutoff serves to retain the stored energy of the cavity. The collar thus helps meet two important experimental needs. It raises the cavity Q factor and it increases the isolation between the cavities. At critical coupling, Q factors of about 25 000 and at an isolation of 105 dB were achieved with this arrangement.

A varactor diode tuning method is used to provide fine cavity tuning while the system is under vacuum. The simplicity of this arrangement, opposed to a complicated vacuum linkage scheme necessary for a mechanical tuner, is quite desirable; however, the penalty for this simplicity is a reduced tuning range. It is convenient to have a wide tuning range mainly to accommodate the shift in the resonant frequency of the cavity as it is evacuated. With a narrow range, it becomes necessary to calibrate carefully the vacuum shift for each different bulb and then to tune carefully to a position which offsets this shift of the resonant frequency. The limitation in range is due to limited varactor diode capacitance range on the one hand, and cavity-Q spoilage on the other. A range of about 80 kHz has been achieved without significant Q reduction.

The principle of varactor tuning is quite straightforward. In the tank circuit approximation of a resonant cavity, a varactor diode, when properly coupled, will introduce an extra capacitance in parallel with the cavity capacitance. As this added contribution varies, the cavity resonant frequency will vary also. The coupling is accomplished by a loop that is completed by the diode. Part of the stored energy in the cavity is stored in the diode by the induced emf around the loop, and it is this fraction which determines the tuning range. However, the diode portion cannot become overly large because then self-resonance effects in the diode loop will spoil the cavity Q. The self-resonance will appear either when the diode capacitance is large or when the loop is very large in area.

This simple model, although illustrating the principle, does not reproduce quantitative results exactly. Apparently there is, in addition, a familiar coupled circuit-pulling effect when the diode loop is near self-resonance.

The varactor diode-loop arrangement is shown in the cavity assembly view of Fig. 2. Of the various designs tested, the one shown seems to meet best the twin requirements of wide tuning range and high Q. The diode loop is placed 2.5 in. from the center on the movable end plate with an orientation which intercepts the maximum number of flux lines of the cavity TE_{011} mode. The varactors are unencapsulated and nonmagnetic (VAS 64 XV, Varian Associates, Bomac Div.).

The components described above are placed inside a vacuum vessel so that (a) a differential vacuum could be maintained in the high-vacuum storage chambers, (b) the problem of bulb and chamber connection would be less acute, and (c) the large storage chamber could be lightweight and easily handled for Teflon coating. The vessel itself was constructed from $\frac{1}{2}$-in.-thick aluminum (Al 6061-T6) with standard vacuum techniques for fabrication. It is 94 in. long at the extreme points, 66 in. o.d. at the main cylindrical body, and 73.5 in. o.d. at the large end cap flange. One end is flanged and made removable to accommodate the inner storage box. The other end contains numerous ports and is connected by two vacuum pipes to the pump and source assembly outside the shields. A manhole is provided to allow entrance into the critical region where the resonant cavities are placed and where the storage chambers are interconnected. Two large ports allow rough tuning of the cavities, a necessary and frequent procedure. Smaller ports are provided for a variety of reasons, but mainly to make the vessel versatile and adaptable to future needs. Two side ports provide an additional working angle into the cavity and storage-bulb regions. To allow easy movement, both the tank itself and its movable end cap are placed on casters, which are guided by a set of rails. The end cap is sealed with a $\frac{1}{2}$-in.-thick Viton O ring which was spliced to the correct groove diameter, and the remainder of the ports is sealed by compression of Pb-In wires of various sizes (indium alloy No. 10, 90% Pb, 10% In, Indium Corporation of America).

Two high-vacuum ion-sublimation pumps evacuate the vessel and the hydrogen storage chambers. One pump (Orb-Ion, Model No. 206, Norton Vacuum Corp.) evacuates the storage-chamber regions

through an aperture defining an appropriate geometrical lifetime of hydrogen atoms, and another pump of the same type evacuates the outer vessel and source chamber. Two 6-in.-diam aluminum pipes connect the pumps through the shields to the vacuum vessel as shown schematically in Fig. 3. Normally, when the source is not running, a pressure of about 2×10^{-8} Torr is maintained in the storage regions and 3×10^{-7} Torr in the outer vessel.

The 6-in.-diam orb-ion pump is rated at 800 liters/sec for air and about twice that high for hydrogen when the pressure is below 10^{-6} Torr, although the speed begins to drop rapidly at pressures of 10^{-5} Torr and higher. Such high pumping speeds are quite necessary because of the large volume of the system and because of anticipated heavy hydrogen fluxes.

Two major pump difficulties emerged: The pumps became saturated under heavy loads of hydrogen flux; and the pump walls began peeling off layers of adhered gas and titanium much sooner than expected. The first problem occurred typically after hydrogen was pumped for about 5–8 h at pressures of above 10^{-5} Torr. The pressure would then begin to rise. Evidently, in this situation, sublimation rates are not fast enough. After a period of time, more loosely bound hydrogen is released from the pump surface than is pumped away. Once this condition develops, a prolonged high-temperature pump bakeout is necessary. This is accomplished by turning off the cooling water to the pump walls and wrapping them in glass fiber insulation while the pump is running. Fortunately, the saturation can be avoided by limiting the hydrogen fluxes so that the source chamber pressure is below about 8×10^{-6} Torr. The second problem, that of wall layer peeling, cannot be avoided, however, and it is serious for one particular case. If in the vertical configuration the closed end of the pump is below the open end, the flakes of peeling wall material will inevitably cause a short circuit between the anode and the grounded body as they fall down into the high-voltage feedthrough assembly. The pump then must be reconditioned (manufacturer's confidential process). Under heavy usage and frequent pressure cycling the peeling phenomena can start in as little as 2–3 mos.

The amplification of the signal from the low-level cavity is accomplished by two amplifiers. The first is a tunnel-diode amplifier (6 stages, 80 dB gain at 1420 MHz, 5 dB noise figure, and manufactured by the International Microwave Corporation, Cos Cob, Conn.). During the course of the experiment it was necessary to increase the gain and a second amplifier was added. This was a transistor amplifier of 20-dB gain (same company).

Magnetic shielding has been the most successful approach for eliminating field gradients which cause relaxation of the stored atoms and for allowing operation of the hydrogen maser at a low static field where variations of the field do not cause sizable changes of the quadratically field-dependent transition frequency.[3] For the large maser also, this approach has been duplicated and a cubical structure to enclose the vacuum vessel magnetically was constructed. Externally the structure measures 10 ft wide $\times$ 9.5 ft high $\times$ 11.5 ft long. Three complete layers of Moly-Permalloy spaced 6 in. apart provide the shielding. When properly demagnetized, the residual magnetic field inside the enclosure is about a thousand times smaller than the ambient field outside and the gradients in the central volume are less than 2×10^{-5} Oe per ft. Satisfactory demagnetization is achieved by passing ac current directly through the vacuum vessel along the azimuthal direction. A transformer arrangement provides currents of 1000 A when the inductive impedance of the shields is canceled appropriately.

V. RESULTS AND INTERPRETATION

Transient operation of the maser is a useful means for extracting information regarding the relaxation processes in the maser system. The measurement of T_2 is possible through the observation of the decay of the stored energy in a cavity after an external pulse has been applied to place the atoms into a radiant state and while the maser is far below threshold for oscillation. In this situation the decay-time constant is equal to T_2 and the initial-signal amplitude is related to T_1.[16]

The procedures for generating the rf pulse and for detecting the signal decay in the studies of the large maser are quite similar to those described by Berg.[16] There are two essential differences: (a) the decay signal is observed on one cavity while the pulse is applied to the other cavity; and (b) the pulse is applied for several seconds to allow a sizable fraction of the stored atoms to be stimulated. Of course, to ensure that threshold conditions do not exist, the amplifier coupling the cavities is removed. In the interpretation of the signals, particularly if amplitude data is used, care has to be taken to account for the fact that the atoms are stimulated only in one region of the system.[25]

Figure 4 shows typical results for the large maser. The confinement time in the system is calculated to be 10 sec. At the low flux position, T_2 is about 3 sec; this is degraded by spin-exchange broadening to 1.5 sec. at high flux. These data together with the relative signal amplitudes at the two flux positions indicate that at high flux there are 10^{14} atoms/sec entering the storage chambers and that, of this total, nearly $\frac{1}{2}$ are in the $F=1$, $M_F=0$ state. This represents the high-

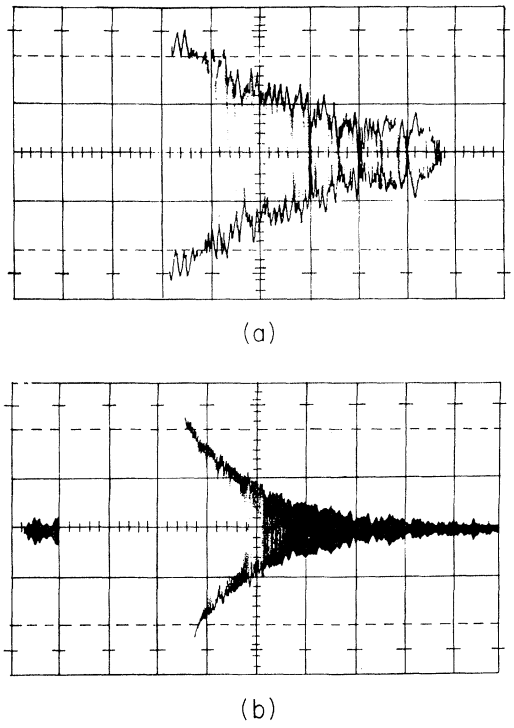

FIG. 4. Decay of pulse-induced emission. The time scale is 1 sec per division. (a) Decay at low flux. (b) Decay at high flux.

est flux levels achieved with the source arrangement used. It was not always possible to obtain such good performance. There seemed to be evidence that the Pyrex walls of the discharge bulb would deteriorate with running time and the maximum flux levels would decrease as a result.

The limitation of the radiation lifetime to 3 sec is a serious handicap for the larger maser. Flow constriction effects emerge at this point since the rate of flow into the driving cavity is about 0.5 sec^{-1}. The factor κ is about 3.5 rather than 1.5 in the case $T_2 = 10$ sec, and ξ, at saturation levels, is of the order of unity rather than of 0.1. The above data indicate that the magnitude of the relaxation rate that is in excess of the sum of spin-exchange and escape rate is about 0.2 sec^{-1}.

Magnetic field gradients are not the cause of the high relaxation rate because as the Larmor frequency increases and becomes greater than the frequency of wall collisions, magnetic relaxation decreases rapidly.[2] The field magnitude for which the Larmor frequency matches the frequency of wall collisions (2.5×10^3 sec^{-1}) is approximately 2 mOe. And, indeed, the signals are quite small at such a field, but they increase steadily and are quite strong at 10 mOe, and do not improve in amplitude or lifetime at 30, 60, or 100 mOe. In fact, the small signal amplitudes at the fields much below 10 mOe are due to the misorientation of the static field from the z direction caused by the residual $\frac{1}{2}$ mOe of the earth's field. Thus, since the above pulse data were taken at a field of 60 mOe, no significant line broadening comes from magnetic relaxations.

The most likely cause of the short lifetimes is the nonadiabatic relaxation of the hydrogen atoms on the wall surfaces generally or perhaps on discrete imperfections on the surfaces. The role that this relaxation mechanism plays in the hydrogen maser is not unambiguously determined. Some workers[16] find that wall relaxation is minor and that the probability for relaxation upon a single bounce is as low as 1×10^{-5}, while others,[5] on the other hand, find a value that is 10 times higher. This particular work seems to indicate that for TFE Teflon, such as used here, the relaxation probability is as high as 10^{-4}. Measurements on a smaller bulb with an identical surface seem to indicate also a figure of that magnitude, although in that case complications associated with the equipment make the interpretation of the relaxation data somewhat difficult.

Specific instances during the course of this experiment of even further degradation of lifetimes were caused by vacuum difficulties. Slight leaks were detected by their effect on the pulse signals. It may be that the residual 0_2-spin exchange,[16] even under the best vacuum conditions achieved here, is causing the excess observed relaxation. However, the improvement has always leveled out even after better base pressures were attained and even after several months of pumping and after the particular leak problems were alleviated. A residual-gas analysis would probably settle the matter, but for lack of appropriate equipment it has not been carried out.

Electromagnetic isolation between the cavities was a serious difficulty with the large-maser system. Initially, only 80 dB of isolation was achieved. Improvement was obtained only when a thicker silver coating was used on the quartz walls of the cavities and when the bulb-neck diameter was reduced from 3 to 2 in. on the uncritical low-level cavity. Further improvement resulted when the rear of each cavity, shown in Fig. 2, was covered with a metal plate after the tuning adjustments were completed. It was helpful also to use only spherical bulbs since the cylindrical variety apparently perturbed the cavity modes in such a way as to couple out more power. With these changes a satisfactory isolation of 105 dB was attained.

Frequency measurements were performed by comparing the signal from the large maser to a reference hydrogen maser signal which was offset in frequency by about 1 Hz through a higher static magnetic field. The period of the slow detected beat frequency was counted on an electronic counter. When the necessary offset corrections

for the second-order Doppler shift and the magnetic field are applied to the period data, and when it is assumed that both masers are tuned for no cavity or spin-exchange frequency pulling, the resulting difference in frequency will be due solely to the difference in the wall collision shifts.

The radiated power in the low-level cavity is estimated to be 4×10^{-11} ergs/sec at low flux and 25 times that at high flux. At a power level of 10^{-10} ergs/sec, the measured frequency instability of the large maser relative to a small reference maser was about 6 parts in 10^{13} for 10-sec averaging times. This result is in agreement with the theory of additive noise contribution to maser frequency instability derived by Cutler and Searle.[30] For 100-sec averaging times, the frequency fluctuations were about 1 part in 10^{13}. In this case, however, it is difficult to compare with theoretical predictions because the laboratory conditions were such that over such long times, environmental perturbations of the reference maser were significant contributors to the observed frequency variations. The principal perturbation appeared to be due to magnetic field variation and caused most of the observed slow-frequency changes. On the other hand, the phase stability of the amplifier loop of the large maser was high enough so that it did not appear to contribute to any sizable frequency drifting and was not a limiting factor.

The requirement of good phase stability for the amplifier loop is clearly exhibited in Eq. (46) by the ϕ term. For a fractional frequency stability of 1×10^{-13}, for example, ϕ must remain constant within 0.1°. Observations of the frequency tuning of the large maser indicate that this sort of phase stability was achieved in the experiment. In addition, there is also the requirement that the noise figure of the amplifier be low as the perturbing noise power in the large-maser case is increased directly by the noise figure factor F of the amplifier. Thus the usual description of thermally induced frequency fluctuations[2,30] in the hydrogen maser can be applied to this case provided kT is replaced by FkT.

The oscillator frequency can still be displaced from ω_0, the density-independent frequency, in the case of the large maser by the power terms which appear in Eq. (50). From a knowledge of the oscillation level, cavity Q factors, amplifier gain, and other factors, it is possible to evaluate the term ξ. This yields for the maximum oscillation level used in the experiment the result that $\xi_{max}=0.3$: and the displacement of the frequency from ω_0 due to these terms when there is no variation of frequency with flux is less than 1 part in 10^{13}. Thus, the power-pulling terms associated with spin-exchange are not detectable in the present measurements. Ultimately, for the full potential accuracies of the large maser, these terms must be measured or their magnitude reduced. For example, a 10% measurement would give the ultimate accuracy of the absolute frequency as 1×10^{-14}. If improvements can be made so that the constriction of flow is less severe, that accuracy could be obtained with even a poorer determination of the ξ terms in Eq. (50). Either approach, direct measurement or the reduction of constriction, can thus be used to remove this new spin-exchange effect from limiting the absolute accuracy of the large maser frequency.

Of great importance to frequency measurements is the amount of broadening that can be introduced by spin-exchange relaxation as the flux is varied to a high position. The greater the broadening, the more pulling there will be at the high flux position and the easier it will be to determine the density-independent frequency ω_0. By using the tuning relationship it can be shown that if the tuning factor T is the ratio of linewidths between high and low flux, and if in the approximately tuned position there is a frequency change Δ when the flux is increased to the high position, then the frequency of the maser oscillator is different from the density-independent frequency by

$$\delta\nu=\Delta/(T-1)\,. \tag{51}$$

If the amount of broadening is small and T is close to unity, one can see that it becomes extremely difficult to determine a tuned position. Also, for a given magnitude of random fluctuations one can set a limit of accuracy of the tuned position from the above relation.

Typically for the small masers the tuning factor T is larger than 2. For the large maser there are two problems. First, the maximum available flux is limited by the discharge source and is below the value of maximum flux allowed for oscillation. Secondly, because of excessive relaxations as noted in the T_2 measurements, the amount of relative broadening is less than it otherwise would be for the same flux range. Under the best conditions heretofore achieved with the large maser, the tuning factor was about 1.7 and was quite adequate. However, during the course of the work the source operation deteriorated somewhat, and in the later measurements a tuning factor of only 1.2 was obtained. Such a low tuning factor was quite troublesome and clearly limited the accuracy of wall measurements.

Three sets of measurements of the large-maser wall shift were obtained. The first set was with the tuning factor of 1.7, and the last two with a tuning factor of 1.2 only. The size of the uncertainties of the latter two determinations indicates the unsatisfactory flux broadening performance.

Under the most favorable conditions achieved during the experiment, the wall shift was found to be smaller than for a small-reference maser bulb by

$(21.1 \pm 0.45) \times 10^{-3}$ Hz,

where the uncertainty in the relative measurement is a standard deviation of the random errors. These errors reflect mainly the uncertainty of the large-maser tuning with the contributing power terms and the inability to measure the magnetic field offset with a negligible error. However, with more statistics and improvements in magnetic field offset determination (the signal to noise of the detected oscillation is presently too low for a sufficiently accurate application of the double resonance technique), a fractional accuracy of 1×10^{-13} should be achievable without difficulty.

It was necessary to carry out a separate series of measurements to determine the absolute value of the reference-maser wall shift, as it appeared immediately that the accepted Teflon values did not seem to agree with the observed data. The results of this study,[9] which included also some temperature dependence observations, give for the reference maser a wall shift (for 31.5 °C) of

$$-(22.5 \pm 0.5) \times 10^{-3} \text{ Hz} .$$

These data, together with temperature corrections and the above determination of the relative wall effects, give for the large maser an absolute wall collision shift (for 26.9 °C) of

$$-(2.3 \pm 0.8) \times 10^{-3} \text{ Hz} .$$

Another series of large-maser measurements was also done, but with a much poorer tuning capability. A tuning factor of only 1.2 was achieved later due to the degradation in the source performance. The average of these results gives $-(2.4 \pm 1) \times 10^{-3}$ Hz for the large-maser wall shift. The extrapolation of the Teflon data of the small bulbs to the large-maser case indicates a shift of -2.8×10^{-3} Hz should be expected. Thus the results overlap the expected value. Full agreement, however, should not be expected as the Teflon surfaces are not of the same type. The small bulbs are FEP Teflon, and the large chamber is coated with TFE Teflon.

This work has demonstrated the feasibility of atomic prestimulation as a method for achieving maser oscillation in a very low filling-factor system. In this case, the system offers the potential of increased absolute accuracy at the expense of a decrease in stability against noise perturbations over short averaging times. Moreover, at longer averaging times of the maser signal the narrower atomic linewidth may prove to be an advantage against flicker noise introduced by cavity tuning drifts.

The effects of wall collisions on the maser frequency have been reduced in this system by the desired order of magnitude. If the wall measurement procedures of conventional masers are carried over to this system, an increase in the accuracy can be expected. A most promising method, particularly suitable for the large maser, is one in which the geometry of the storage box can be changed while maintaining the same identical surface area. The resulting variation in the collision rate could determine the wall effect of the large maser independently of the limiting wall errors associated with the small storage bulbs of the conventional hydrogen masers.

The apparatus developed here can be readily adapted to achieve a deuterium maser oscillator. The system is large enough to accept the larger deuterium resonance cavity and a measurement of the deuterium hyperfine frequency via the maser method is being done in this laboratory.

ACKNOWLEDGMENTS

The authors wish to thank D. Kleppner for numerous helpful discussions, D. Wineland for calculation of cavity tuning effects, and the hydrogen maser group at Harvard for generous help during the course of the experimental work. Design of the apparatus involved principally F. Robie, who helped design the magnetic shields and J. Blandino, who helped plan the vacuum system.

---

*Work supported by the Office of Naval Research.

†Present Address: Joint Institute for Laboratory Astrophysics, Boulder, Colo. 80302.

[1]H. M. Goldenberg, D. Kleppner, and N. F. Ramsey, Phys. Rev. Letters 5, 361 (1960).

[2]D. Kleppner, H. M. Goldenberg, and N. R. Ramsey, Phys. Rev. 126, 603 (1962).

[3]D. Kleppner, H. C. Berg, S. B. Crampton, N. F. Ramsey, R. F. C. Vessot, H. E. Peters, and J. Vanier, Phys. Rev. 138, A972 (1965).

[4]B. S. Mathur, S. B. Crampton, D. Kleppner, and N. F. Ramsey, Phys. Rev. 158, 14 (1967).

[5]R. Vessot, M. Levine, L. Cutler, M. Baker, and L. Mueller, Proceedings of the Twenty-second Annual Symposium on Frequency Control (U.S. Army Electronics Command, Ft. Monmouth, N.J., 1968), p. 605; Frequency 6, 11 (1968).

[6]R. Vessot *et al.*, IEEE Trans. Instr. Measur. IM-15, 165 (1966).

[7]A. O. McCoubrey, Proc. IEEE 55, 805 (1967).

[8]R. Beehler *et al.*, IEEE 54, 301 (1966).

[9]E. Uzgiris and P. W. Zitzewitz, Proceedings of the Twenty-third Annual Symposium on Frequency Control (U.S. Army Electronics Command, Ft. Monmouth, N.J., 1969), p. 284.

[10]D. Brenner (private communication).

[11]By "filling factor" we mean the square of the atom-averaged z component of the oscillatory field divided by the square of the total rf field amplitude averaged over the cavity volume.

[12]P. L. Bender, Phys. Rev. 132, 2154 (1963).

[13]E. E. Uzgiris and N. F. Ramsey, in Polarisation Matière et Rayonnement, edited by Societé Francaise de Physique (Presses Universitaires de France, Paris, 1969), p. 493; in Ref. 5, p. 452; IEEE J. Quantum Electron. QE-4, 563 (1968).

[14]N. F. Ramsey, Molecular Beams (Oxford University Press, New York, 1956), Chap. VI.

[15]In Ref. 12, for example, the radiation rate of an atom is displayed in terms of its oscillating magnetization component.

[16]H. C. Berg, Phys. Rev. 137, A1621 (1965).

[17]H. C. Berg (private communication).

[18]S. B. Crampton, Phys. Rev. 158, 57 (1967).

[19]This is derived in Ref. 3. For a sphere of radius R, $d=\frac{4}{3}R$, and for a cylinder of radius R and length L, $d=2L\times(1+L/R)^{-1}$, and for the general case $d=4V/A$, where A is the surface area and V is the volume.

[20]C. P. Slichter, Principles of Magnetic Resonance (Harper and Row Publishers, Inc., New York, 1963), Chap. V.

[21]U. Fano, Rev. Mod. Phys. 29, 74 (1957).

[22]S. B. Crampton, H. G. Robinson, D. Kleppner, and N. F. Ramsey, Phys. Rev. 141, 55 (1966).

[23]This relaxation rate is given in Refs. 3 and 4 as $\gamma_H = T_H^{-1} = (T_1)^{-1}_{\text{s.e.}} = n\sigma V_r$, where n is the hydrogen density, σ is the spin-exchange cross section, and V_r is the mean relative velocity.

[24]L. C. Balling, R. J. Hanson, and F. M. Pipkin, Phys. Rev. 133, A607 (1964). Also the spin-exchange shift parameter λ and the exchange cross section σ are defined in Ref. 18, Eqs. (21) and (22).

[25]E. E. Uzgiris, Ph. D. thesis, Harvard University, 1968 (unpublished).

[26]For a circuit-element description of cavities, see, for example, R. Beringer in Technique of Microwave Measurements, edited by C. G. Montgomery (Boston Technical Publishers, Inc., Lexington, Mass., 1964), p. 286. The circuit analog approach for the two-cavity maser system was first suggested by D. Wineland.

[27]J. C. Slater, Rev. Modern Phys. 18, 441 (1946); J. C. Slater, Microwave Electronics (D. Van Nostrand Co., Inc., Princeton, N. J., 1950).

[28]A. E. Siegman, Microwave Solid-State Masers (McGraw-Hill Book Co., New York, 1964), p. 264.

[29]Reference 2, Eq. (22).

[30]L. S. Cutler and C. L. Searle, Proc. IEEE 54, 136 (1966).

PHYSICAL REVIEW A VOLUME 1, NUMBER 2 FEBRUARY 1970

Quantum-Mechanical Amplification and Frequency Conversion with a Trilinear Hamiltonian

Daniel F. Walls*†
Physics Department, Harvard University, Cambridge, Massachusetts 02138
and
Richard Barakat
Division of Engineering and Applied Physics, Harvard University, Cambridge, Massachusetts 02138
(Received 23 June 1969)

A description of the parametric amplifier and frequency converter is presented without introducing the classical (i.e., parametric) approximation for the pumping field. Constants of the motion are found which reduce the solution of the Schrödinger equation to the diagonalization of a matrix. This diagonalization is accomplished numerically, and the eigenvalues and eigenfunctions of a system with fixed energy are calculated. The time-dependent behavior of the mean number of photons in the amplified or frequency up-converted field is presented. The time evolution of the probability distributions is illustrated. The technique is extended to the problem of coherent spontaneous emission from a system of N two-level atoms interacting with the radiation field where both the atomic system and the radiation field are quantized.

1. INTRODUCTION

Recently, there have been great advances made in the construction of light amplifiers and frequency converters. These devices are based on the coupling of light waves in nonlinear dielectric crystals such as $LiNbO_3$.[1,2] A photon from an intense monochromatic laser beam, the pump, couples